

User Support Office use only

Date:

Date:

Proposal for Nuclear Physics Experiment at RI Beam Factory (RIBF NP-PAC-12, 2013)

Title of Experiment	Study of density dependence of the symmetry energy with the measurements of charged pion ratio in heavy RI collisions		
Category	<input checked="" type="checkbox"/> NP experiment <input type="checkbox"/> Detector R&D <input type="checkbox"/> Construction <input type="checkbox"/> Update proposal (Experimental Program: NP____-____)		
Experimental Devices	<input type="checkbox"/> GARIS <input type="checkbox"/> RIPS <input checked="" type="checkbox"/> BigRIPS <input type="checkbox"/> Zero Degree <input type="checkbox"/> SHARAQ <input checked="" type="checkbox"/> SAMURAI		
Detectors	<input type="checkbox"/> DALI2 <input type="checkbox"/> GRAPE <input type="checkbox"/> EURICA		

Co-spokesperson :

Name	William G. Lynch		
Institution	NSCL, Michigan State University		
Title of position	Professor		
Address	1 Cyclotron, East Lansing, MI 48824-1321, USA		
Tel	+1-517-333-6319	Fax	+1-517-353-5967
Email	lynch@nscl.msu.edu		

Co-spokesperson :

Name	Tetsuya Murakami		
Institution	Department of Physics, Kyoto University		
Title of position	Lecturer		
Address	29-25 Kitabatake Kohata Uji, Kyoto 611-0002, Japan		
Tel	+81-75-753-3866	Fax	+81-75-753-3887
Email	murakami@scphys.kyoto-u.ac.jp		

Your proposal should be sent to User Support Office (UserSupportOffice@ribf.riken.jp)

Co-spokesperson :

Name	Tadaaki Isobe		
Institution	RIKEN, Nishina Center		
Title of position	Research Scientist		
Address	RIBF BLDG318, RIKEN Hirosawa 2-1, Wako, Saitama, Japan		
Tel	+81-48-467-4174	Fax	+81-48-462-4464
Email	isobe@riken.jp		

Co-spokesperson :

Name	Betty Tsang		
Institution	NSCL, Michigan State University		
Title of position	Professor		
Address	1 Cyclotron, East Lansing, MI 48824-1321, USA		
Tel	+1-517-333-6386	Fax	+1-517-353-5967
Email	tsang@nscl.msu.edu		

Beam Time Request Summary:

Please indicate requested beam times of $T_{\text{User-Tuning}}$ & $T_{\text{User-Data Run}}$ only. T_{BigRIPS} and **Total** times will be given by RIKEN.

Total Beam Time	T_{BigRIPS} : Tuning time with BigRIPS for secondary beam settings	(User Support Office use only)	days
	$T_{\text{User-Tuning}}$: Tuning time for users' own equipment and/or detectors using primary / secondary beams		days
	$T_{\text{User-Data Run}}$: Beam-time for data runs		days
TOTAL		(User Support Office use only)	days

Beam summary

Primary Beams:

Particle	^{238}U	Energy	345	(E/A MeV)	Intensity	>10	(pnA)
----------	------------------	--------	-----	-----------	-----------	-----	-------

Particle	^{124}Xe	Energy	345	(E/A MeV)	Intensity	>10	(pnA)
----------	-------------------	--------	-----	-----------	-----------	-----	-------

Secondary Beams:

RI Beams			Beam-on-Target Time for DATA RUN
Isotope	Energy (E/A MeV)	Intensity(/s)	Days
^{132}Sn	300	$1*10^4$	3 +2 (debugging)
^{124}Sn	300	$1*10^4$	3
^{132}Sn	200	$1*10^4$	3
^{124}Sn	200	$1*10^4$	3
^{108}Sn	300	$1*10^4$	3
^{112}Sn	300	$1*10^4$	3
^{108}Sn	200	$1*10^4$	3
^{112}Sn	200	$1*10^4$	3

Readiness

Estimated date ready to run the experiment	September, 2014
Dates which should be excluded, if any	Christmas, Dec 21-30

Summary of Experiments

As the first measurements using the SAMURAI-Time Project Chamber (TPC), we propose to measure the pions, nucleon, triton and ^3He yield ratios and flows from the collisions of the following beam + target combinations: $^{132}\text{Sn}+^{124}\text{Sn}$, $^{124}\text{Sn}+^{112}\text{Sn}$, $^{108}\text{Sn}+^{112}\text{Sn}$ and $^{112}\text{Sn}+^{124}\text{Sn}$ with beams at incident energies of $E/A=200$ MeV and 300 MeV. These experiments with the SAMURAI TPC and the NEBULA neutron array will provide important constraints on the EoS for neutron-rich matter at supra-saturation densities. We plan to compare observables from the $\pi^- - \pi^+$, neutron-proton and t - ^3He isospin doublets, which theoretically are predicted to display selective sensitivity to the symmetry energy. We will use this data to disentangle the symmetry energy effects from those coming from neutron-proton effective masses and isospin dependent in-medium cross sections and obtain independent constraints on all these quantities. The $^{132}\text{Sn}+^{124}\text{Sn}$ ($N/Z=1.58$) collision will be the most neutron rich system while $^{108}\text{Sn}+^{112}\text{Sn}$ ($N/Z=1.20$) will be the most neutron deficient system that have been measured as these heavy isotope beams can only be produced in sufficient intensities at RIKEN. The two systems provide the largest differences in asymmetries and thus the best sensitivity to the symmetry energy term in the equation of state. The intermediate reactions $^{124}\text{Sn}+^{112}\text{Sn}$ and $^{112}\text{Sn}+^{124}\text{Sn}$ provide information about the in-medium cross sections and also reference reactions where extensive measurements have been performed at lower energies.

Detailed Description of the proposed experiment

I. Experimental Objectives:

The nuclear Equation of State (EoS) is a fundamental property of nuclear matter that describes the relationships between the energy, pressure, temperature, density and isospin asymmetry $\delta=(\rho_n-\rho_p)/\rho$ for a nuclear system [Dan02]. It can be divided into a symmetric matter contribution that is independent of the isospin asymmetry and a symmetry energy term, proportional to the square of the asymmetry [Lat01, Lat04]. This second term describes the dependence of the EoS on asymmetry. Investigations that provide an improved understanding of this term will also provide an improved understanding of masses [Dan03], fission barriers, energies of isovector collective vibrations [Kli07, Dan03], the thickness of the neutron skins of neutron-rich nuclei [Bro00], and an improved understanding of the role of isovector modes in fusion and strongly damped collisions.

Macroscopic quantities of asymmetric nuclear matter exist over a wide range of densities in neutron stars and in type II supernovae [Lat01]. Experimental information about the EoS can help to provide improved predictions for neutron star observables such as stellar radii and moments of inertia, crustal vibration frequencies [Lat04, Vil04], and neutron star cooling rates [Lat04, Ste05] that are currently being investigated with ground-based and satellite observatories. For many of these observables, the absence of strong constraints on the symmetry energy term of the EoS engenders major theoretical uncertainties. The recent observation of a twice solar mass neutron star Pulsar J1614-2230 [Dem10] places significant constraints on the maximum energy densities, pressures and baryon chemical potentials achieved at the centers of neutron stars.

The goal of determining the EoS at densities in the vicinity of 2-3 ρ_0 has been a major motivation for many X-ray observations of neutron stars because the radii of most neutron stars are strongly sensitive to the EoS at this density. Analyses of these data have shown the potential of such observations to provide some constraints on the EoS, but current uncertainties in the radiation transport and other dynamics in the neutron star surface contribute significant uncertainties to the constraints that can be currently drawn from such observations [Oze05, Ste13, Sul11]. We propose to investigate the EoS at supra-saturation densities and obtain constraints on the EoS of neutron-rich matter that are urgently needed to check whether constraints drawn from astronomical observations can be supported by laboratory measurements.

II. Constraining the density dependence of the symmetry energy from heavy ion collisions

The total energy per nucleon (i.e. the Equation of State (EoS)) of cold nuclear matter can be written as the sum of a symmetry energy term and the energy per nucleon of symmetric matter,

$$E(\rho, \delta) = E_0(\rho, \delta=0) + E_\delta; \quad E_\delta = S(\rho)\delta^2, \quad (1)$$

where the asymmetry $\delta = (\rho_n - \rho_p) / \rho$, ρ_n , ρ_p and ρ are the neutron, proton and nucleon number densities, and $S(\rho)$ describes the density dependence of the symmetry energy term, E_δ . Measurements of isoscalar collective vibrations, collective flow and kaon production in energetic nucleus-nucleus collisions have constrained the equation of state for symmetric matter, $E_0(\rho, \delta=0)$, for densities ranging from saturation density to five times saturation density [Dan02, Fuc06, You97]. The extrapolation of the EoS to neutron-rich matter depends on $S(\rho)$, which has few experimental constraints [Bro00] until recently.

IIa. Present constraints at sub-saturation densities

Many recent efforts to constrain the density dependence of the symmetry energy have focused on its behavior near saturation density. There, one may expand the symmetry energy, $S(\rho)$, about the saturation density, ρ_0 ,

$$S(\rho) = S_0 + \frac{L}{3} \left(\frac{\rho - \rho_0}{\rho_0} \right) + \frac{K_{sym}}{18} \left(\frac{\rho - \rho_0}{\rho_0} \right)^2 + \dots \quad (2)$$

where L and K_{sym} are slope and curvature parameters at ρ_0 . The slope parameter, L , is related to P_0 , the pressure from the symmetry energy for pure neutron matter at saturation density as follows:

$$L = 3\rho_0 \left. \frac{dS(\rho)}{d\rho} \right|_{\rho_0} = \left[\frac{3}{\rho_0} \right] P_0. \quad (3)$$

The symmetry pressure, P_0 , provides the baryonic contribution to the pressure in neutron stars at saturation density [Ste05], where the energy of symmetric matter, $E_0(\rho, \delta=0)$, contributes no pressure, and it is also related to the neutron skin thickness (δR_{np}) of neutron rich heavy nuclei including ^{208}Pb [Hor01, Typ01]. In the last few years, elastic and inelastic proton scattering [Zen10, Tam11], measurements of collective structures such as the Giant Monopole Resonance [Li07] and the Pygmy Dipole Resonance [Kli07] in neutron-rich nuclei, and measurement of reaction observables such as isospin diffusion [Tsa04], collective flow [Rus11], neutron/proton emission [Fam06], and fragment isotopic ratios [Tsa01, Igl06] have provided initial constraints on the density dependence of the symmetry energy at sub-saturation densities [Li08, Tsa08, Tsa12]. Cross-comparisons of these constraints were provided in ref. [Tsa12]. By combining the constraints on $S_0 = 30.2$ to 33.8 MeV from the Pygmy Dipole Resonance (PDR) data [Kli07] with constraints on L from [Tsa08], one can obtain tentative bounds on the allowed symmetry energy at sub-saturation density. The bounded region in Figs. 1 represents the current status of our understanding of the symmetry energy at sub-saturation density. New measurements and calculations will have a considerable impact and changes and improvements in such constraints will be expected. More information on this subject can be found in ref. [Tsa12].

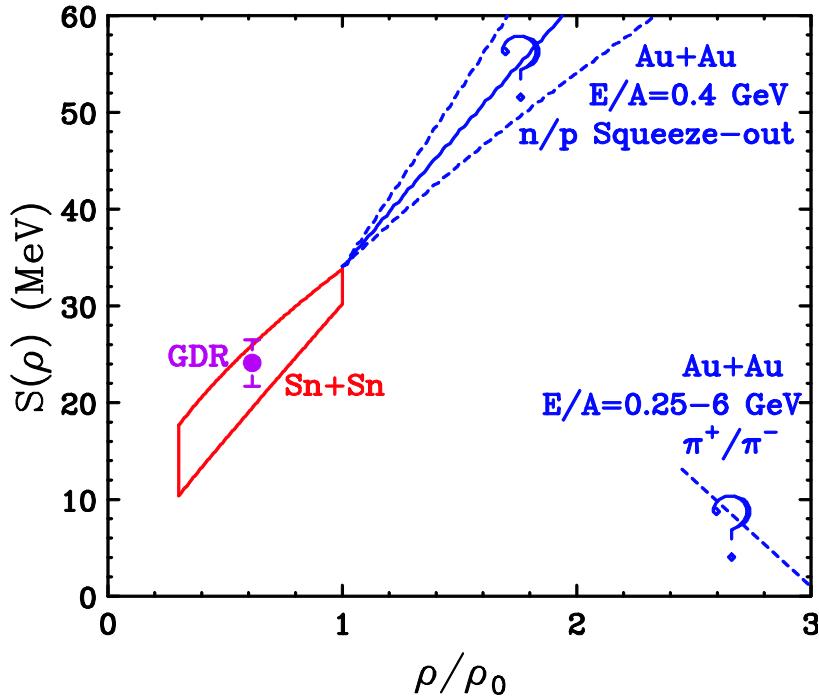


Fig. 1: Density dependence of the symmetry energy obtained from heavy ion reactions. The limits to the enclosed region at sub-saturation nuclear matter density are obtained from Sn+Sn collision data assuming $S_0=30.1$ and 33.8 MeV. The dotted line in the lower right corner of the supra-saturation density region represents initial constraints analyzed from the measurements of π^+/π^- yield ratio data from Au+Au collisions [Xia08, Rei07] and comparison to IBUU04 transport model. The solid and dashed lines near the top of the graph represent the constraint obtained by comparing neutron and proton elliptical flow from Au+Au collisions [Rus11].

IIb. Extension of present constraints to supra-saturation densities: relevance to neutron stars

In contrary to the sub-saturation density region, there is very little data in the supra-saturation density region. The dotted curve from $\rho \sim 0.4$ to 0.5 fm^{-3} represents the symmetry energy consistent with a recent theoretical analysis [Xia08] of the π^+/π^- yield ratio data for Au+Au reactions from Ref. [Rei07]. These analyses suggest that the symmetry energy at $\rho/\rho_0 \geq 2.5$ is much smaller than it is at saturation density and that the symmetry energy reaches a maximum at densities between 1-2 times the saturation density. This conclusion, however, is based on the comparison to a single set of data that has not been optimally chosen to constrain the symmetry energy at supra-saturation densities as discussed in Sections III and IV. The dotted-dashed curve in the upper right hand side of this figure represents the density dependence of the symmetry energy that best agrees with comparisons of proton and neutron elliptical flows reported in Ref. [Rus11]. Similar to the constraints from the pion measurements, these constraints from n-p elliptical flow were obtained from measurements that were not specifically designed to constrain the density dependence of the symmetry energy. The tentative constraints obtained using π^+/π^- yield ratio data from Au+Au collisions [Xia08,Rei07] can be significantly improved by the measurements at RIKEN discussed in Sections III and IV of this proposal.

Constraints on the symmetry energy at supra-saturation density from the proposed measurements can be highly relevant to neutron stars, and may be more relevant to calculations of neutron star radii than the difference between the neutron and proton matter radii of ^{208}Pb , a quantity that probes the symmetry energy at sub-saturation densities [Hor01]. Fig. 2 compares the correlation between the baryonic pressure at saturation density (left panel) or twice saturation density (right panel) and the neutron star radius [Lat01]. For neutron star radii in the region of $R=9\text{-}13$ km, the correlation between the neutron star radius and the pressure at saturation density is relatively weak. In contrast, the correlation at twice saturation density is much sharper; constraints on the EoS at supra-saturation densities can have a significant influence on predictions of neutron star radii.

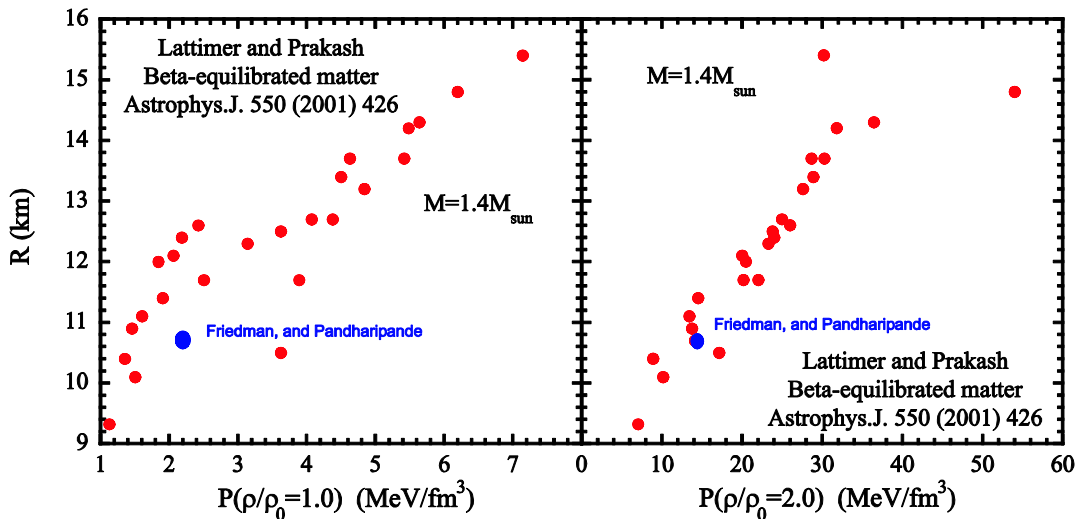


Fig. 2: Correlation between the neutron star radius and the baryonic pressure at saturation density (left panel) or twice saturation density (right panel). Adapted from Ref. [Lat01]

III. Experimental Probes using the SAMURAI TPC

The main focus of the present section will be on the measurements that can be performed at using the proposed TPC. In this beam time request we focus specifically on comparisons of π^+ and π^- production and how this production depends on the n-z asymmetry of the colliding system and on the incident energy. In addition to pions, the TPC also detects and identifies light charged particles such as proton, tritons and ^3He . When the TPC is coupled with a highly efficient neutron

detector, such as the NEBULA array, at RIKEN, it will be possible to measure neutron-proton spectral double ratios. In this section, we discuss measurements of pion production [Li02], neutron vs. proton emission and differential flow [Li02] and triton and ^3He emission, that can provide significant constraints on the density dependence of the symmetry energy, the neutron-proton effective mass splitting and the isospin dependence of the in-medium nucleon-nucleon cross-sections at supra-saturation density. The observables discussed below probe a range of densities that can be controlled by selecting the incident energy and impact parameter of the collision. While incident energies of up to $E/A=350$ MeV and densities in excess of $2\rho_0$ can be explored with stable beams at RIKEN, we focus on the unique capabilities at RIKEN to collide more asymmetric rare isotope beams, such as ^{132}Sn or ^{108}Sn at incident energies of $E/A=300$ and 250 MeV, which can provide increased sensitivity to the symmetry energy.

III.a) Pion production

Investigations of pion production in nucleus-nucleus collisions provide unique opportunities to establish meaningful constraints on the density dependence of the symmetry energy at high densities $\rho > \rho_0$. Calculations predict that the relative concentrations of neutrons and protons in the dense interior of a central nucleus-nucleus collision reflect the pressure of the symmetry energy, which is greater for a “stiffer” symmetry energy term with stronger density dependence [Li97, Bar01]. The left side of Fig. 3 shows the ratio of the neutron/proton central densities for $^{132}\text{Sn}+^{124}\text{Sn}$ collisions at $E/A = 400$ MeV. It decreases with time for strongly repulsive symmetry energy, while increasing in time for much softer symmetry energy. This decrease for the stiff symmetry energy stems from the larger repulsive potential energy of the stiff symmetry energy at higher density.

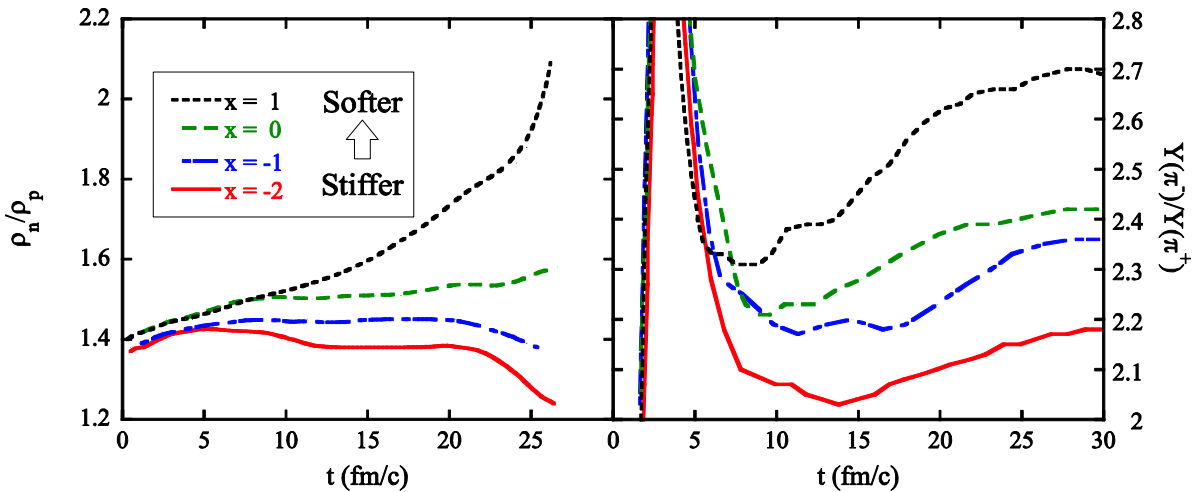


Fig. 3: (Left panel) The dashed and solid lines show the predicted ratio of neutron over proton densities at $r_{\text{cm}}=0$ as a function of time for symmetry energies that range from weakly repulsive or slightly attractive ($x = 1$) to strongly repulsive ($x = -2$). (Right panel) The dashed and solid lines show the corresponding pion single ratios $Y(\pi^-)/Y(\pi^+)$ [Li02].

Pions are largely produced at these incident energies by Δ resonance production and decay. Consequently, π^- and π^+ production rates are strongly correlated with the n-n and p-p collision rates at maximum density, respectively. In the BUU calculations of ref. [Yon05], the larger ρ_n/ρ_p for much less repulsive symmetry energies (left panel) results in larger $Y(\pi^-)/Y(\pi^+)$ yield ratios in the right panel of Fig. 3 [Yon05] (right panel). The asymptotic values of these ratios at large times are the predictions for the $Y(\pi^-)/Y(\pi^+)$ yield ratios that are compared to experiment. It is this effect that was exploited to provide the constraints from Au+Au collision shown on the lower right hand side of Fig. 1. Compared to the influence of the symmetry energy on the ratios of pionic energy spectra discussed below, the influence of the symmetry energy on the ratio

of total π^- to total π^+ production is comparatively weak, and it may be sensitive to other effects such as the treatment of the optical potential for pions produced in the collision.

A significantly stronger sensitivity to the density dependence of the symmetry energy can be obtained by dividing the energy spectra of positive and negative pions. Fig. 4 shows the ratio of the differential multiplicities of negative pions over positive pions as a function of the pion energy in the center of mass for the $^{132}\text{Sn}+^{124}\text{Sn}$ system at $E/A=300$ MeV [Jun13]. Even though the range of density dependences of the symmetry energy explored in Fig. 3 is much larger than that explored in Fig. 4, the variation of ratio of pion spectra in Fig. 4 is much larger, decreasing with E_{cm} by a factor of about 4.4 for the stiffer symmetry energy, and only by a factor of 1.6 for the softer symmetry energy.

Pion absorption and rescattering reduce the sensitivity of pion production with incident energy. Calculated sensitivities of pion production to the symmetry energy are significant at energies $E/A \leq 0.5$ GeV below the free nucleon-nucleon production threshold [Qin05, Bar05]; and increase as the incident energy decreases. For example, the right panel in Fig. 4 shows the corresponding ratios as $E/A=120$ MeV. Here, one finds the ratio for the stiff symmetry energy $\gamma=2.0$ to be 3 times larger at low energy, but 2 times smaller at a higher energy of 60 MeV. The request to explore pion production at $E/A = 200$ MeV reflects a compromise between counting rate and the importance of observing this sensitivity.

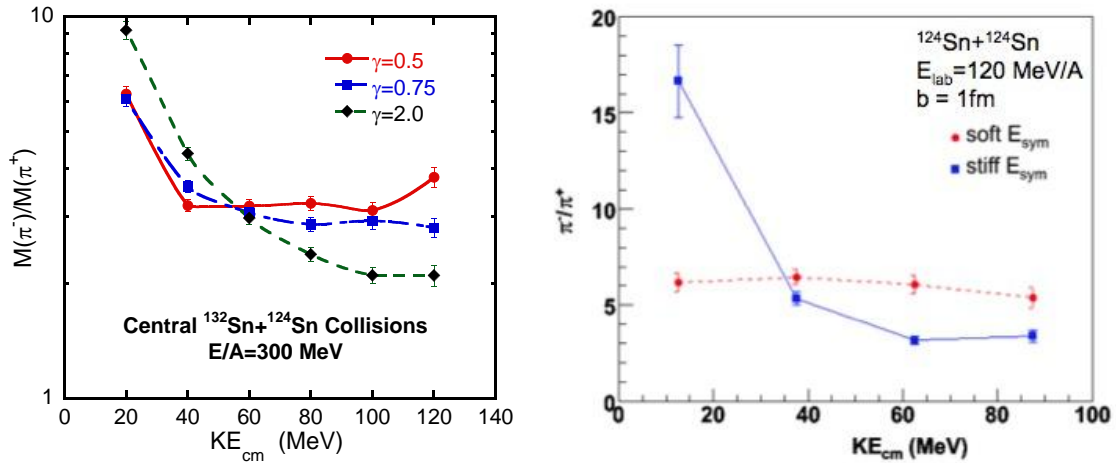


Fig. 4 Ratios of π^- over π^+ center of mass energy spectra are shown for central ($b=1$ fm) $^{132}\text{Sn}+^{124}\text{Sn}$ collisions at $E/A = 300$ MeV. The circles, squares and diamonds correspond to BUU calculations for symmetry energy functions with potential terms that depend on density as ρ^γ [Hong and Danielewicz].

Experimentally, the double yield ratio [Yon05] obtained by comparing the yield ratio from two reactions, is a more selective observable to probe the symmetry energy. This is also demonstrated with transport calculations by [Yon05]. The Coulomb “effect” on the relative production of positive and negative pions has been clearly demonstrated [Fra85]; thus, it is important to unambiguously distinguish the effects of Coulomb and symmetry potentials. This can be accomplished by explicitly comparing pairs of reactions with the same total charge but very different isospin asymmetries. With the Sn isotope reaction pairs, one can remove the Coulomb effects as well as differences in the detection efficiencies for negative and positive pions by constructing pion double ratios as in [Yon05]

$$R(\pi^-/\pi^+) = [Y(\pi^-; ^{132}\text{Sn}+^{124}\text{Sn}) \cdot Y(\pi^+; ^{112}\text{Sn}+^{112}\text{Sn})] / [Y(\pi^+; ^{132}\text{Sn}+^{124}\text{Sn}) \cdot Y(\pi^-; ^{112}\text{Sn}+^{112}\text{Sn})] \quad (5)$$

Similar to the single ratio, predictions for the double ratio, shown in Fig. 5, display a strong sensitivity to the density dependence of the symmetry energy [Yon05].

The tentative constraint from the π^- to π^+ ratios shown as dotted line in Fig. 1 comes from the experimental measurements of one system, Au+Au at incident energy at 0.4 to 1.2 GeV. It is very sensitive to Coulomb effects and to

differences between the π^- to π^+ detection efficiencies. The Au+Au system has both a large asymmetry and Coulomb mean field potentials. For this set of measurements, we propose to explore measure pion production in a system with larger asymmetry using $^{132}\text{Sn}+^{124}\text{Sn}$ collisions and isolate the symmetry energy effects by contrasting this data with data obtained with the $^{124}\text{Sn}+^{112}\text{Sn}$ and $^{108}\text{Sn}+^{112}\text{Sn}$ systems, which have the same Coulomb effects. To minimize possible effects coming from differences in the detection efficiencies of π^- and π^+ , we require measurements of different reactions in the same setup. Thus, we propose to perform $^{132}\text{Sn}+^{124}\text{Sn}$ and $^{124}\text{Sn}+^{112}\text{Sn}$ with the ^{238}U primary beam and $^{112}\text{Sn}+^{124}\text{Sn}$ and $^{108}\text{Sn}+^{112}\text{Sn}$ with the ^{124}Xe primary beam. The range of asymmetry $\delta=(N-Z)/A$ of these beams allows the influence of the symmetry energy, which scales as the square of the asymmetry of the total system, to be clearly isolated. To reduce the uncertainties in the predictions for pion production, additional measurements of the collective flows of nucleons and light clusters at RIKEN will be simultaneously be performed. These other measurements will be part of a broader program to constrain transport properties such as the nucleon effective masses and in-medium cross sections that also influence the pion production [Bar05]

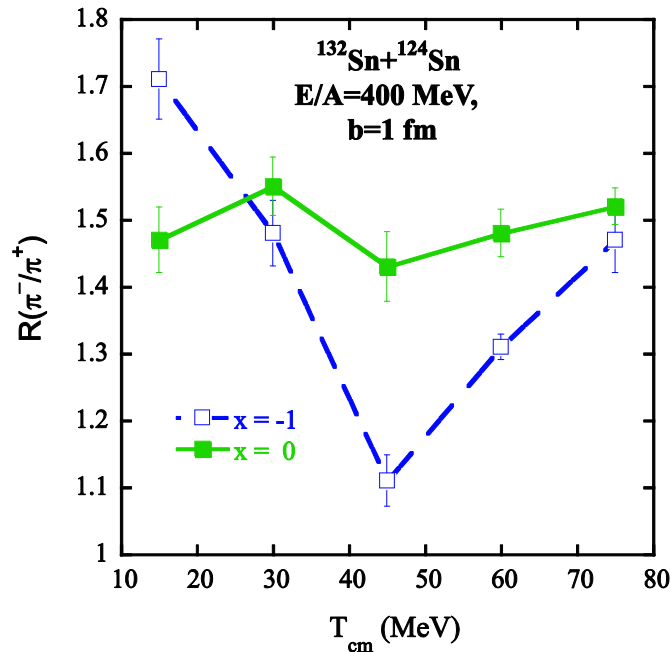


Fig. 5: The solid and open squares show the predicted pion double ratio, $R(\pi^-/\pi^+)$, as a function of the pion center of mass kinetic energy, for weakly ($x=0$) and strongly ($x=-1$) density dependent symmetry energies [Yon05].

III.b) Neutron – proton, t – ^3He ratios and differential flows

In this section, we briefly mention studies of neutron to proton (n/p) and triton to ^3He ($t/^3\text{He}$) ratios and differential flows, at RIKEN. We note that investigations of the symmetric matter EoS required measurements of a variety of observables to obtain independent constraints on the symmetric matter EoS, on the nucleon-nucleon cross-sections and on the momentum dependence of the mean field [Dan02]. Similarly, a range of measurements, including pion *and nucleon or light cluster* observables, will be required to obtain independent constraints on the symmetry energy, the neutron and proton effective masses and the isospin dependence of the nucleon-nucleon cross sections.

Both n/p and $t/^3\text{He}$ ratios and differential flows [Fam06, Li97, Li05] strongly reflect the density and momentum dependencies on symmetry energy. The momentum dependence means that comparisons of neutron-proton spectral ratios and flows display a strong sensitivity to the difference between the neutron and proton effective masses. This difference depends on the energy of the reaction, on the densities achieved in the reactions and is roughly proportional to

the n-z asymmetry of the collision. Figure 6 shows predictions for the n/p and $t^3\text{He}$ ratios as function of transverse momentum for central Au+Au collisions at $E/A=400$ MeV [DiT10]. Here, $p_t/p_{\text{proj}}=1$ when the emitted particles are moving with the velocity of beam in the center of mass. The similarity of the two ratios should not be surprising; the two are directly related in the coalescence approximation, which should be fairly accurate at such energies. Both ratios are understandably larger at large momentum in the case where $m_n^* < m_p^*$ than in the opposite case where $m_n^* > m_p^*$. This simply reflects the fact the nucleon with a lower effective mass will be more readily accelerated to large momentum. Smaller variations in n/p and $t^3\text{He}$ ratios have been recently measured for collisions at lower incident energies ($E/A=120$ MeV) at the NSCL/MSU. With the large acceptance of the SAMURAI TPC, we will be able measure $t^3\text{He}$ ratios, and if we include the NEBULA array, we will be able to obtain complementary n/p ratios as well.

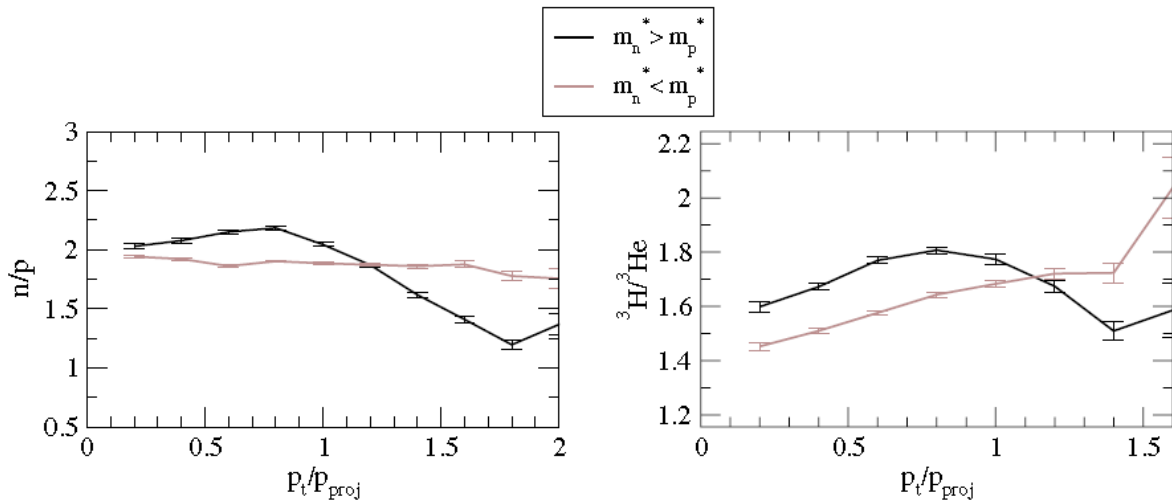


Fig. 6: Results from transport calculations adapted from Ref. [DiT10]. Left panel; The points indicate ratios of calculated n/p differential multiplicities (spectra) as a function of the momentum of the nucleons in the CM. system. The dark (black) points indicate the values obtained by assuming the effective mass ratio $m_n^*/m_p^* > 1$ and the lighter (brown) points indicate the corresponding values when $m_n^*/m_p^* < 1$. Right panel: The corresponding $t^3\text{He}$ ratios are shown using the same labeling convention as in the left panel.

IV. Plan of proposed measurements.

We propose to perform these measurements by installing a Time Projection Chamber in the SAMURAI Dipole magnet. In 2009, we successfully proposed this TPC and its experimental program to the 5th meeting of the RIBF program advisory committee as an equipment proposal. Successful proposals to the U.S. Department of Energy and to Grant in Aid program in Japan provided the funds for the TPC and its electronics. The SAMURAI TPC is now in its final stages of construction and testing and is briefly described in Section V of this proposal. Commissioning for the TPC was approved at the 5th meeting of the RIBF program advisory committee. In the following, we propose the first series of experiments to be performed following the successful commissioning of the SAMURAI TPC at the RIBF facility.

The scientific objectives of this proposal are:

- Measure the differential multiplicities of positive and negative pions for central $^{132}\text{Sn}+^{124}\text{Sn}$ and $^{108}\text{Sn}+^{112}\text{Sn}$ collisions at $E/A=300$ MeV and 250 MeV and construct single (e.g. $M_{132+124}(\pi^-)/M_{132+124}(\pi^+)$ or $M_{108+112}(\pi^-)/M_{108+112}(\pi^+)$) and double spectral ratios (e.g. $M_{108+112}(\pi^+) \cdot M_{132+124}(\pi^-) / [M_{132+124}(\pi^+) \cdot M_{108+112}(\pi^-)]$). These will be explored as a function of the pion energy in the center of mass system.
- At 300 MeV, we have enough statistics that we can compare the ratios of pions emitted in the reaction plane to those emitted out of the reaction plane. Pions emitted out of the reaction plane will in general have less nuclear material to penetrate (as the impact parameter b is not zero) and will more clearly

reflect the initial pion production rates. Other angular cuts will allow us probe the influence of Coulomb effects from the projectile target residues.

- Compare these measured ratios to corresponding theoretical calculations and obtain constraints on the density dependence of the symmetry energy at twice saturation density.
- Explore the dependence of pion ratios as a function of incident energy in order to explore the predicted sensitivities to incident energy as manifested in nature.
- Obtain complementary information on the density dependence of the density and momentum dependence (effective masses) of the symmetry energy from ratios of the differential multiplicities of tritons and ^3He particles. This will be measured at the same times as the pion measurements discussed above.
- Take complementary differential multiplicity data for protons and neutrons (with NEBULA) and assess the feasibility of a later high statistics measurement focused on comparisons of neutron and proton differential multiplicities and flows.

In the proposed measurements, ^{132}Sn or ^{108}Sn beams will pass through an upstream scintillator near the entrance of the SAMURAI dipole, then pass through a foil window that separates the vacuum in the beam line from the TPC gas. The beam will collide with a 200 mg/cm^2 ^{124}Sn or ^{112}Sn target mounted on a target ladder that positions them 1 cm upstream from the entrance window of the field cage of the TPC. Particles produced in the target enter the TPC through its $7\text{cm}\times 7\text{cm}$ upstream window. A trigger scintillator array consisting of scintillator paddles placed outside of thin-walled enclosure of the TPC, will provide an external trigger. The external trigger will require the observation of a beam particle entering the TPC, the absence of a high Z projectile residue exiting the TPC and the observation of mid-rapidity charged particles produced by the collision. The TPC electronics also allows a fast trigger condition based on the number of pads with signals, if more precise information about the multiplicity proves useful to better select events for data recording. A typical trigger will accept events with the highest 30% of charged particle multiplicity, corresponding roughly to an impact parameter of approximately $b_{\text{trig}} < 6\text{ fm}$, corresponding to a cross section of about 1.1 b. Central collisions will be defined as $b_{\text{cent}} < 3.5\text{ fm}$ corresponding to a cross section of about 0.4 b.

In our rate estimates, we assume that we will run the SAMUARI TPC can run at beam intensities for the requested particle of about 5×10^3 beam particles/s, with or without contaminants. (We hope that we can actually run at 10^4 /s.) Table 1 gives expected beams rates and contaminants predicted by LISE calculations performed in support of this proposal. A minimum bias impact parameter of 6 fm translates into an reaction rate of slightly more than 5 per second and a central collision rate of about 2 per second. Both are expected to be much less than the maximum data rate of 500/s achievable in the TPC data acquisition. For the higher beam energy of 300 MeV/u, we can obtain ratios of energy spectra with selected azimuthal or polar angle cuts or cuts on rapidity. At the lower incident energy, we will not have the statistics for such cuts, we expect the higher sensitivity of the spectral ratios to compensate for the reduced and we should be able to provide angle integrated spectra similar to those shown in Fig. 4.

Table 2 gives the beam times and the expected data rates for each reaction on this proposal

primary beam	RIB	rate /s	energy MeV/A	tgt	π^+ mult	π^- mult	π^+ rate /s	π^- rate /s	hours	π^+ total (10^3) cts	π^- total (10^3) cts
^{238}U	^{132}Sn	5000	300	^{124}Sn	.14	.5	.05	.24	72	13	62

^{238}U	^{124}Sn	5000	300	^{112}Sn	.24	.4	.1	.2	72	26	55
^{238}U	^{132}Sn	5000	200	^{124}Sn	.01	.06	.004	.03	72	1.1	7.4
^{238}U	^{124}Sn	5000	200	^{112}Sn	.02	.05	.008	.025	72	2.1	6.6
^{124}Xe	^{108}Sn	5000	300	^{112}Sn	.24	.4	.1	.2	72	26	55
^{124}Xe	^{112}Sn	5000	300	^{124}Sn	.20	.45	.8	.2	72	19	55
^{124}Xe	^{108}Sn	5000	200	^{112}Sn	.02	.05	.008	.025	72	2.1	6.5
^{124}Xe	^{112}Sn	5000	200	^{124}Sn	.02	.06	.007	.026	72	1.9	6.6

In addition to these beam times, we require 48 hours for debugging and adjusting the trigger at beginning of the experiment.

V. Development of the SAMURAI Time Projection Chamber (TPC):

V.a) SAMURAI Dipole

With a pole diameter of 2 m and magnet gap of 80 cm, the SAMURAI dipole is somewhat smaller than the HISS magnet (2.1m pole diameter and 1 m magnet gap) that housed the EOS TPC at the LBL Bevalac [Wie91]. The magnet can be rotated to optimize detection of particles at nearly any polar angle. Our initial program will have the dipole oriented perpendicular to the beam. Table 3. gives some relevant parameters of the SAMURAI dipole and Table 4 lists the relevant parameters of the SAMURAI TPC design to fit inside the SAMURAI dipole.

SAMURAI Dipole Specifications	
Magnet Type	H
Maximum Rigidity	7 Tm
Pole Diameter	2m
Central Field	0.4-3 T (at the center)
Magnet Gap	0.88 m – 0.8 m with vacuum chamber

Table 3: Parameters of the SAMURAI Dipole.

SAMURAI TPC Parameters	
Pad Plane Area	1.34 m x 0.86 m
Number of pads	12096 (112 x 108)
Pad size	12 mm x 8 mm
Drift distance	53 cm
Pressure	1 atmosphere
Gas composition	90% Ar+10% CH ₄
Gas gain	3000
E field	120 V/cm
Drift velocity	5 cm/ μ s
dE/dx range	Z=1-8, π , p, d, t, He, Li-O
Two track resolution	2.5 cm
Multiplicity limit	200

Table 4: Relevant parameters of the SAMURAI TPC.

V.d) Ancillary neutron detectors (NEBULA):

A large-area neutron detector (NEBULA) has been developed at the RIBF facility for invariant mass measurements using the SAMURAI TPC. While its inclusion is not essential to meet the central scientific objectives of the present proposal, placing NEBULA near $\theta_{cm} \sim 90^\circ$ (in the center of mass) would allow us to construct n/p spectra ratios for comparison to the $t^3\text{He}$ ratios that will be provided by the TPC itself. Including it in the proposed experiments would also allow us to take data which could help us to understand the difficulties in analyzing the response of NEBULA to high neutron multiplicity events and to develop procedures to analyze them. If these studies prove promising, a later high intensity experiment with an internal field cage in the TPC would be proposed. Such an experiment would provide precise data that would be complementary to the pion measurements proposed here.

VI. Readiness

The SAMURAI TPC is in its final stages of construction. Current plan is to ship the TPC in December of 2013 from MSU to RIKEN when the GET electronics is delivered to RIKEN. We will spend the first six months to install the GET electronics and fully test the TPC. If an experimental program is approved for the TPC, we will start installing the TPC inside the SAMURAI chamber during the summer shut-down in 2014. We plan to do a commission run of 3 days in the Fall of 2014. We have no preference in the choice of specific commissioning heavy ion beam as long as the charge of the beam is around 50, similar to the Sn isotopes we plan to use as secondary beams. We request a month between the commissioned run and the first experiment to allow time for us to correct problems that we diagnosed during the commissioning. As the TPC is a very complicated device and takes two to three months to set up. During that time, other SAMURAI experiments cannot be run. It is important that enough beam time be allocated to run a complete experimental program. The SAMURAI-TPC collaboration is large with a lot of students and postdocs as well as experienced researchers. We have the manpower to handle complicated analysis to extract different aspects of the physics. Unlike most RIKEN proposals, we would like to request beam time for a comprehensive measurements with many different reactions rather than many small scale experiments by individual members.

V.b) Current Status of SAMURAI TPC

An exploded drawing of the SAMURAI TPC together with photographs of various parts is shown in Figure 7. The electric drift field in the TPC is vertical and is provided by a field cage with vertical panels that are set 5 cm back from the pad plane. The 53 cm drift distance considers the space required within the 80 cm gap for the electronics and various mechanical structures, and for the anode structure.

The field cage, pad and wire planes and chamber enclosure have been assembled. We are currently testing the pad and wire planes with pulsers using STAR TPC electronics. We expect to attach the field cage to the top plate with its pad plane and wire planes early this summer. The whole assembly will be installed inside the enclosure and we plan to conduct tests with minimum ionizing particles this summer. Progress on the construction of the TPC has been reviewed recently by the Department of Energy committee on January 16, 2013. The review panel concurred with our plans to ship the TPC to RIKEN at the end of 2013.

V.c) TPC electronics:

The SAMURAI TPC will be read out with the Generic Electronics for TPCs (GET), which have been under development by a collaboration based in SACLAY, GANIL, Bordeaux and MSU. After several prototypes, the GET is scheduled for fabrication in 2013 and we expect to receive the GET readout modules required for the SAMURAI TPC towards the end of 2013. In the mean time, we have been testing the performance of the GET prototype electronics with a

smaller BRAHMS TPC. At the end of the summer, we plan to test prototypes of GET electronics modules on the SAMURAI TPC at MSU before the SAMURAI TPC is shipped to RIKEN at the end of 2013.

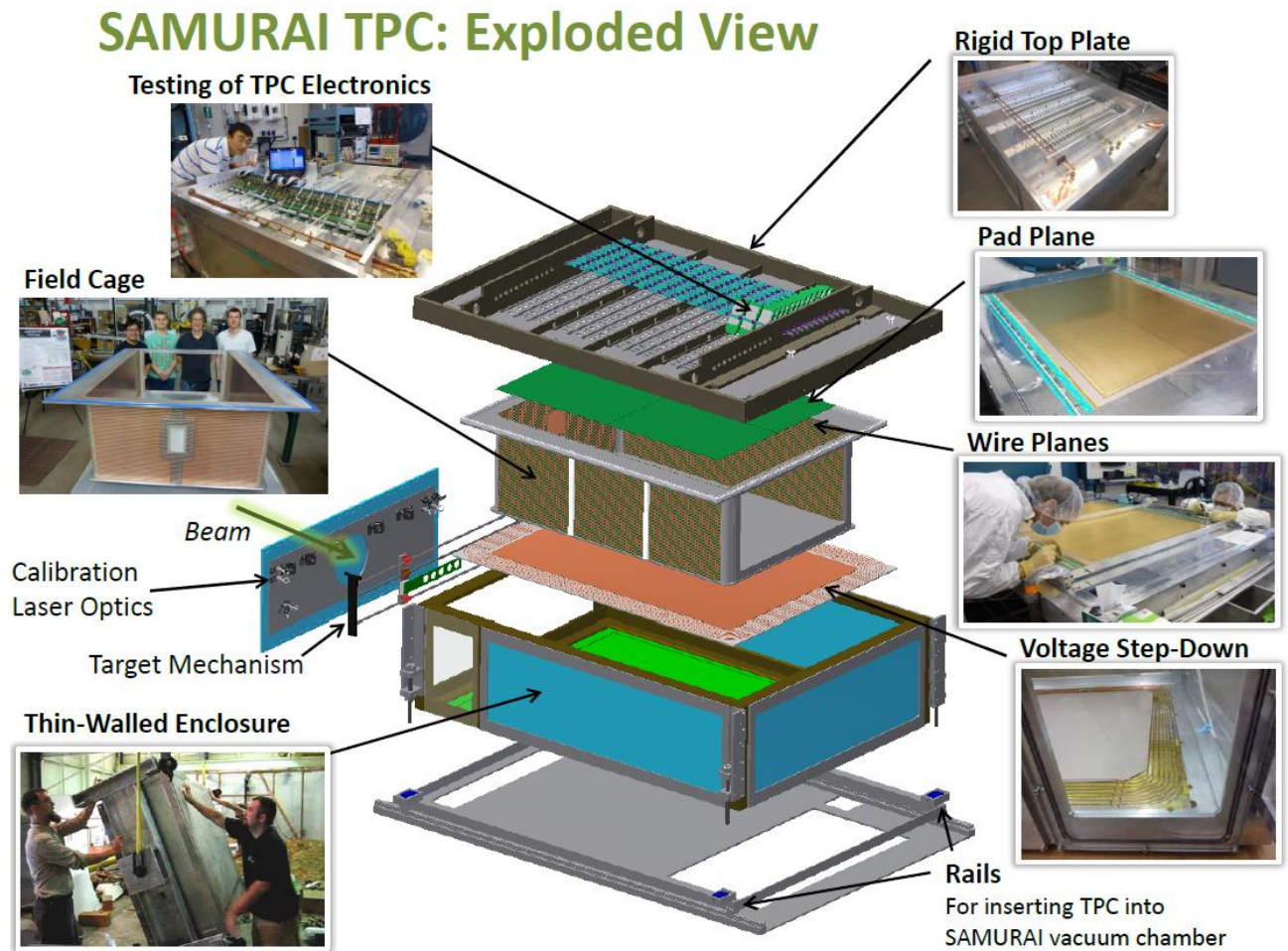


Fig. 7: Exploded drawing of the TPC with pictures showing various components of the target.

References:

- [Bar01] V. Baran, M. Colonna, M. Di Toro, V. Greco, Phys. Rev. Lett. 86, 4492 (2001)
- [Bar05] V. Baran, M. Colonna, V. Greco, M. Di Toro, Phys. Rep. 410, 335 (2005).
- [Bro00] B.A. Brown, Phys. Rev. C 43, R1513(1991)
- [Car10] A. Carbone et al., Phys. Rev. C 81, 041301 (2010).
- [Dan02] P. Danielewicz, R. Lacey, W.G. Lynch, Science 298, 1592 (2002)
- [Dan03] P. Danielewicz, Nucl. Phys. A 727, 233 (2003).
- [Dan08] Pawel Danielewicz and Jenny Lee, AIP Conf. Proc. 1423, 29 (2012) and references therein
- [Dem10] P. B. Demorest, T. Pennucci, S. M. Ransom, M. S. E. Roberts and J. W. T. Hessels, Nature, 467, 1081 (2010).
- [DiT10] M. DiToro et al, J. Phys. G. 37, 083101 (2010)
- [Fam06] M.A. Famiano et al., Phys. Rev. Lett. 97, 052701 (2006).
- [Fra85] K. A. Frankel et al., Phys. Rev. C 32, 975 (1985).
- [Fuc06] C. Fuchs, Prog. Part. Nucl. Phys. 56 (2006) 1.

- [Hor01] C.J. Horowitz and J. Piekarewicz, Phys. Rev. C 64, 062802(R) (2001).
- [Igl06] J. Igljo et al., Phys. Rev. C **74**, 024605 (2006).
- [Jun13] Jun Hong and Pawel Danielewicz, private communications, (2013).
- [Kli07] A. Klimkiewicz et al, Phys. Rev. C 76, 051603 (2007).
- [Koh10] Z.Kohley et al., Phys. Rev. C 82, 064601 (2010).
- [Lat01] J.M. Lattimer, M. Prakash, Ap. J. 550, 426 (2001)
- [Lat04] J.M. Lattimer, M. Prakash, Science 304, 536 (2004)
- [Li02] B.A Li, Phys. Rev. Lett. 88, 192701 (2002)
- [Li05] B.A. Li, L.W. Chen, Phys. Rev. C 72 (2005) 064611.
- [Li07] T. Li et al., Phys. Rev. Lett. 99, 162503 (2007).
- [Li97] B.A. Li, C.M. Ko, Z. Ren, Phys. Rev. Lett. 78, 1644 (1997)
- [Li08] Bao-An Li, Lie-Wen Chen, Che Ming Ko, Phys. Rep. 464 (2008) 113.
- [LRP07] <http://www.sc.doe.gov/np/nsac/docs/Nuclear-Science.Low-Res.pdf>.
- [Oze05] F. Özel, Nature 441, 1115-1117(29 June 2006)
- [Qin05] Qingfeng Li, et al., , J. Phys. G: Nucl. Part. Phys. **31** (2005) 1359–1374
- [Rei07] W. Reisdorf, et al., FOPI Collaboration, Nucl. Phys. A 781 (2007) 459.
- [Rus11] P. Russotto et al., Phys. Lett. B697 (2011) 471.
- [Ste05] A.W. Steiner, M. Prakash, J.M. Lattimer, P.J. Ellis, Phys. Rep. 411, 325 (2005)
- [Ste13] A.W. Steiner et al., ApJ Lett. 765, 65 (2013).
- [Sul11] Suleimanov et al, ApJ 742, 122 (2011).
- [Tam11] A. Tamii et al., Phys. Rev. Lett. 107, 062502 (2011)
- [Ter08] S. Terashima, et al., Phys.Rev.C**77**, 024317 (2008)
- [Tsa01] M.B. Tsang, W.A. Friedman, C.K. Gelbke, W.G. Lynch, G. Verde, H.S. Xu, Phys. Rev. Lett. 86, 5023 (2001)
- [Tsa04] M.B. Tsang, et al., Phys. Rev. Lett. 92, 062701 (2004)
- [Tsa09] M. B. Tsang, et al., Phys. Rev. Lett. 102, 122701 (2009).
- [Tsa12] M.B. Tsang et al, Phys. Rev. C 86, 015804 (2012)
- [Typ01] S. Typel, B.A. Brown, Phys. Rev. C 64 (2001) 027302.
- [Vil04] Adam R. Villarreal and Tod E. Strohmayer, ApJ, 614, L121 (2004).
- [Wie91] H. Wieman et al., Nucl. Phys. A 525, 627 (1991).
- [Xia08] Zhigang Xiao, et al., arXiv:0808.0186 (2008)
- [Yon05] Gao-Chan Yong, Bao-An Li, Lie-Wen Chen, nucl-th/0512067 (2006).
- [You97] D. H. Youngblood, H. L. Clark, and Y.-W. Lui, Phys. Rev. Lett. 82, 691 (1999)
- [Zen10] J. Zenihiro, et al., Phys. Rev. C 82, 044611 (2010)